The Study of Copper Adsorption from Aqueous Solution Using Crosslinked Chitosan Immobilized on Bentonite

Nurak Grisdanurak,[1] Siripor Akewaranugulsiri,[2] Cybelle Morales Futalan,[3] Wan-Chi Tsai,[4] Chi-Chuan Kan,[5] Che-Wei Hsu,[6] Meng-Wei Wan[5]

[1]*National Center of Excellence for Environmental and Hazardous Waste Management, Thammasat University, Pathumthani 12120, Thailand*
[2]*National Center of Excellence for Environmental and Hazardous Waste Management, Chulalongkorn University, Bangkok 10330, Thailand*
[3]*Department of Environmental Engineering, University of Philippines-Diliman, Quezon City, Philippines 1800*
[4]*Department of Medical Laboratory Science and Biotechnology, Kaohsiung Medical University, Kaohsiung, 80708, Taiwan*
[5]*Department of Environmental Engineering and Science, Chia Nan University of Pharmacy and Science, Tainan 71710, Taiwan*
[6]*Department of Emergency Medicine, Sijhih Cathay General Hospital, New Taipei City 22174, Taiwan*

Received 9 March 2011; accepted 25 August 2011
DOI 10.1002/app.35541
Published online in Wiley Online Library (wileyonlinelibrary.com).

ABSTRACT: Batch experiments were performed to investigate the adsorption of Cu(II) from aqueous solution using noncrosslinked and crosslinked chitosan immobilized on bentonite (CIB). Crosslinking agents such as epichlorohydrin (ECH), glutaraldehyde (GLA), and ethylene glycol diglycidyl ether (EDGE) were utilized to improve the chemical and mechanical properties of the adsorbent. The effect of contact time, pH, and initial concentration on the adsorption capacity was determined. The adsorption capacities of the adsorbents are arranged in the following order: CIB-EDGE > CIB-ECH > CIB >> CIB-GLA. Langmuir and Freundlich equations were used to analyze the isotherm data. Equilibrium studies showed that CIB, CIB-EDGE, and CIB-ECH correlated well with the Langmuir model while CIB-GLA fits well with the Freundlich model. Kinetics of Cu(II) adsorption was best described by the pseudosecond-order equation, which indicates that chemisorption is the rate-limiting step. In the desorption study, more than 92 and 75% of Cu(II) could be recovered from CIB-EDGE and CIB-ECH beads using HCl solution (pH 1) agitated for 120 min. J Appl Polym Sci 000: 000–000, 2012

Key words: bentonite; adsorption; chitosan; crosslinking; isotherm

INTRODUCTION

Heavy metals like copper have been widely used in industrial areas such as mining activities, metal cleaning facilities, petroleum refining, and fertilizer manufacturing.[1] Without proper management and disposal of waste effluents, heavy metals can contaminate the environment, especially the groundwater. Copper, Cu(II), is considered an essential nutrient in trace amount but when ingested at high levels, it can cause adverse health effects such as hemolytic anemia, corneal opacity, and Wilson's disease.[2,3]

Conventional treatment methods utilized in heavy metal removal are membrane separation, electrodeposition, chemical precipitation, ion exchange, and reverse osmosis. These technologies are effective but have high operational and maintenance costs and are inefficient in removing heavy metals in dilute solutions.[4] Adsorption is an alternative treatment method, where several studies have focused in finding efficient, low-cost adsorbents such as banana pith,[5] agricultural wastes,[6] chitin, and chitosan.[1,2,4] Chitosan is a product of the partial deacetylation of chitin, which has several valuable properties such as being nontoxic, polycationic, biocompatible and biodegradable. It is well known to be an excellent adsorbent because it contains hydroxyl (—OH) and amino ($—NH_2$) groups that serve as metal binding sites.[1] However, chitosan has a low surface area, with weak chemical and mechanical properties. Therefore, physical and chemical modifications are necessary to overcome these limitations.

Physical modification allows the expansion of the chitosan polymer chain, which decreases its crystallinity and causes the accessibility of its binding sites. Providing a proper and inexpensive material to be used as an immobilization support for chitosan

Correspondence to: M.-W. Wan (peterwan@mail.chna.edu.tw).
Contract grant sponsor: Taiwan National Science Council; contract grant number: NSC 99-2221-E-041-017.

would assist in lowering the quantity of chitosan needed in the treatment process.[7,8] There are several studies that have investigated on potential support materials for chitosan such as sand,[7,9] bentonite,[10,11] alumina,[12] PVC beads,[13] calcium alginate beads,[14] and ion-exchange resin.[15] Among the adsorbents, chitosan immobilized in bentonite is one of the cheapest materials and has a high efficiency in removing heavy metals.[8,10,16] On the other hand, chemical modification such as sulfonation, grafting, blending, carboxymethylation, and crosslinking are utilized to improve mechanical strength, chemical stability, and hydrophilicity, to prevent dissolution in dilute acidic medium, and to enhance its selectivity for metal adsorption. Among the chemical methods, crosslinking has received much attention due to its simple procedure and ability to form macromolecular structure for a variety of applications.[17] Commonly used crosslinking agents are epichlorohydrin (ECH), glutaraldehyde (GLA), and ethylene glycol diglycidyl ether (EDGE).[1,18] Previous batch studies on chitosan and its derivatives utilized either physical or chemical modification but never in combination. The present study will apply both physical modification through chitosan immobilized on bentonite (CIB) and chemical modification using crosslinking agents such as ECH, GLA, and EDGE.

This study examines the removal of Cu(II) ions from aqueous solution using noncrosslinked and crosslinked CIB beads. The noncrosslinked and crosslinked CIB beads were characterized using BET surface area analysis, TGA and XRD. The effect of parameters, such as initial concentration, contact time, and pH, on the adsorption capacity was determined. The equilibrium adsorption data was analyzed using Langmuir and Freundlich models. Kinetic experimental data were evaluated using pseudofirst-order and pseudosecond-order equations. This study will determine the probability of crosslinked CIB beads as a possible material for permeable reactive barriers (PRBs) for the treatment of contaminated groundwater.

MATERIALS AND METHODS

Chemicals and equipment

Low molecular weight chitosan ($C_{12}H_{24}N_2O_9$) produced from crab shells with deacetylation degree of 75–85% and bentonite ($Al_2O_3 \bullet 4SiO_2 \bullet H_2O$) were purchased from Sigma-Aldrich (KGaA, Germany). The following crosslinking agents: epichlorohydrin (ECH) with 99% purity, ethylene glycol diglycidyl ether (EDGE) with 50% purity, and glutaraldehyde with 50% purity were procured from Sigma-Aldrich (Germany). Copper sulfate ($CuSO_4$), hydrochloric acid (37% fuming), and sodium hydroxide (NaOH) were obtained from Merck Germany. All reagents used were of analytical grade. Deionized (DI) water was used to prepare all reagent solutions.

A Channel Precision Oven model DV452 220V was used in drying the adsorbent. A BT-350 YIH shaker bath was used for the batch studies. The amount of Cu(II) in the filtrate was measured using inductively coupled plasma optical emission spectrometry (ICP-OES) Perkin–Elmer DV2000 Series. The specific surface area of chitosan, bentonite, CIB-ECH, CIB-EDGE, and CIB-GLA was measured using BET-N_2 adsorption GEMINI 2360 Micrometrics. X-ray diffraction (XRD) analysis was performed using a Bruker D8 Series with a slow scan at $0.3^\circ\ s^{-1}$ in 2θ range of 2°–15°. Thermogravimetric analysis of chitosan, bentonite, and CIB was performed using a Perkin–Elmer Pyris diamond thermomechanical analyzer.

Preparation of chitosan immobilized on bentonite

Chitosan, 5.0 g, were dissolved in 300 mL of 5% (v/v) HCl under vigorous stirring for 2 h. After chitosan dissolution, 100 g of clay (bentonite) was added into the solution and stirred for 3 h at 25°C. The chitosan-clay solution was neutralized with 1*N* NaOH (pH 13) that was added in a dropwise method until the chitosan has precipitated.[5] The chitosan-bentonite beads was filtered and washed with DI water to remove excess NaOH. The CIB adsorbent was dried in the oven at 65°C for 24 h or until the weight becomes constant. After grinding the particles, called CIB, they were passed through ASTM sieve size #35 and #45. CIB with bead size range of 0.35–0.50 mm was utilized.

Preparation of crosslinked chitosan immobilized on bentonite bead

An equimolar 1 : 1 of chitosan to EDGE, ECH, and GLA were prepared. About 4.578 mL of EDGE, 1.162 mL of ECH, and 2.650 mL of GLA were added into the chitosan-bentonite solution. The CIB solution was stirred continuously at 55°C for 3 h on addition of EDGE, at 45°C for 2 h on addition of ECH, and at 50°C for 6 h on addition of GLA.[19,20] The crosslinked CIB was neutralized, filtered, washed, dried, and sieved similar to the method used for CIB. The crosslinked CIB was designated as CIB-ECH, CIB-EDGE, and CIB-GLA, using ECH, EDGE, and GLA, as crosslinkers, respectively.

Batch adsorption studies

Effect of pH and initial concentration

Batch experiments were carried out using 2.5 g of the adsorbent beads, added in 125 mL Erlenmeyer

flasks containing 30 mL of Cu(II) solution. The solution was agitated using a reciprocal shaker bath at 50 rpm for 4 h at 25°C. The effect of pH (1.0–4.0) and initial concentration (100–2000 mg L^{-1}) on the removal efficiency and adsorption capacity were determined. The adjustment of pH was done using 0.1*N* of NaOH and 0.1*N* HCl. The solution was filtered using Whatman #40 filter paper. The filtrate was analyzed using ICP-OES using the wavelength of 324.75 nm for Cu(II). The percent removal of Cu(II) ion from the solution at any time t is calculated using eq. (1):

$$\text{Percentage adsorption} = \frac{(C_0 - C)100}{C_0} \quad (1)$$

where C_0 and C are the initial and final Cu(II) concentration (mg L^{-1}), respectively.

The adsorption capacity, q_e is given by eq. (2):

$$\text{Adsorption capacity}, q_e = \frac{(C_0 - C)V}{W} \quad (2)$$

where V is the volume of the metal solution (mL), and the W is the weight of the adsorbent used (g).

Kinetic studies

The kinetic studies were carried out using 2.5 g adsorbent beads in 30 mL of Cu(II) solution at pH 4 with initial concentration of 500–2000 mg L^{-1}. The flasks were stirred using 50 rpm at predetermined time intervals (1 min to 2 h). The solution was filtered, and the Cu(II) concentration in the filtrate was measured.

Isotherm studies

The isotherm studies were conducted using 2.5 g adsorbent beads placed in 30 mL of Cu(II) solution with an initial concentration ranging from 100 to 2000 mg L^{-1} at pH 4. The flasks were agitated for 24 h at 50 rpm at 25°C.

Regeneration studies

In regeneration studies, 2.5 g of adsorbent (CIB-ECH and CIB-EDGE) was added to 30 mL of Cu(II) solution with an initial concentration in the range of 100–2000 mg L^{-1} at pH 4. The solution was agitated for 12 h using a shaker bath. Then the solution was filtered and the concentration of Cu(II) was analyzed.

After the first adsorption cycle, the Cu(II)-loaded adsorbent was agitated in a shaker bath for 2 h using tap water (pH 7) and HCl solution (pH 1 and pH 3). The solution was filtered, and the amount of desorbed Cu(II) ions were analyzed. The regenerated adsorbent was again subjected to a second adsorption cycle. This is for confirmation of reusability and stability of the adsorbent.

TABLE I
Characteristic of Adsorbent Beads Analyzed by BET N_2 Adsorption–Desorption Analysis

Adsorbent beads	Surface area (m^2 g^{-1})	Pore volume (m^3 g^{-1})	Average pore diameter (nm)
Bentonite	94.28	0.0113	5.84
Chitosan	3.40	<0.0001	6.41
CIB	39.17	0.0041	5.02
CIB-ECH	38.96	0.0039	6.21
CIB-EGDE	20.18	0.0002	7.33
CIB-GLA	13.45	<0.0001	8.33

RESULTS AND DISCUSSION

Specific surface area analysis

The characterization of the surface area of chitosan, bentonite, CIB, CIB-EDGE, CIB-ECH, and CIB-GLA was listed in Table I. According to the International Union of Pure and Applied Chemistry (IUPAC) classifications, the pore diameters can be divided into three categories: macropores ($d > 50$ nm), mesopores (2 nm $< d <$ 50 nm), and micropores ($d <$ 2 nm). Based on the results, chitosan, bentonite, and crosslinked CIB beads are mesoporous. Table I illustrates that chitosan exhibited the least surface area (3.40 m^2 g^{-1}), whereas bentonite has the largest surface area (94.28 m^2 g^{-1}). Combining bentonite and chitosan to form CIB beads resulted to surface area values in between bentonite and chitosan (48.81 m^2 g^{-1}). On addition of ECH, EGDE, and GLA further reduced the surface area of adsorbent beads in the order of 38.96, 20.18, and 13.45 m^2 g^{-1}, respectively. The surface area values are arranged in the following order: bentonite > CIB ~ CIB-ECH > CIB-EDGE > CIB-GLA > chitosan. It is observed that the surface area decreases with a decrease of pore volume. The inferior properties of CIB and its crosslinked forms in comparison to bentonite were due to the hydroxylated edge–edge interaction of the silicate layers forming hydrogen bonds with another silicate hydroxylated group.[21] In addition, the hydroxyl groups from crosslinking agents form hydrogen bonds with the silicate hydroxylated edge groups of bentonite and the hydroxyl groups of chitosan.

Figure 1 shows the nitrogen adsorption–desorption isotherm of chitosan, CIB, and bentonite. In Figure 2, the adsorption–desorption isotherm of (a) CIB-ECH, (b) CIB-EDGE, and (c) CIB-GLA are displayed, respectively. Based on the figures, the plot of bentonite, CIB, CIB-ECH, CIB-EDGE, and CIB-GLA can be well fitted with type IV adsorption isotherm, which indicates a porous adsorbent material

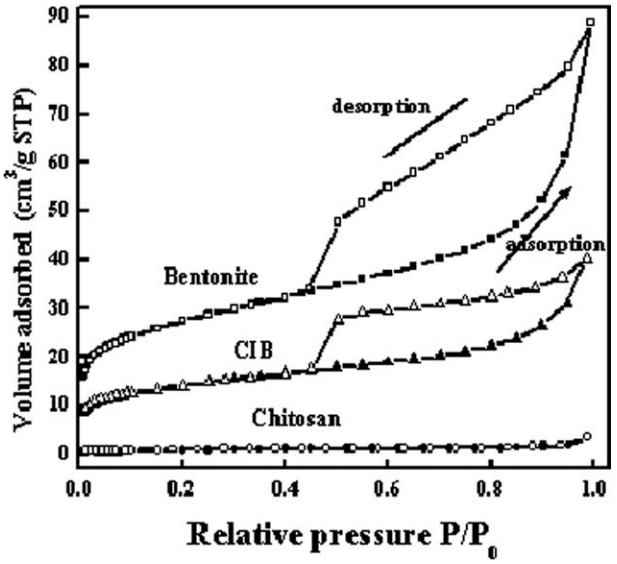

Figure 1 Isotherm plot of N_2 adsorption and desorption on bentonite, CIB, and chitosan.

with strong adsorbate–adsorbent interactions. On the other hand, chitosan displays a type II isotherm, which refers to a nonporous material.

TG analysis

The thermogravimetric curves of chitosan, bentonite, and CIB are shown in Figures 3–5, respectively. In Figure 3, the TG curve of chitosan is composed of two degradation stages. The first stage is due to loss of adsorbed water observed around 40–120°C with a weight loss of 12%. The second major weight loss of 84% was observed around 220–550°C. Chitosan was burnt out completely at 560°C.

In Figure 4, the thermogravimetric profile of bentonite is illustrated, which is composed of two stages. The first weight loss of 12% was observed at 40–130°C that is attributed to evaporation of adsorbed water. The second weight loss of 9% occurred around 450–700°C, which is due to the loss of structural hydroxyl group of bentonite.[22] In Figure 5, the decomposition profile of CIB is similar to that of bentonite. The CIB profile is composed of two weight loss stages, which were observed in the range of 40–130°C and 250–700°C. The first major weight loss of 12% is due to adsorbed water. On the other hand, the second weight loss of 11.1% is composed of the decomposition of both chitosan and bentonite. Around 560°C, the chitosan would be burnt out completely from CIB. Based on the degradation profiles, about 3.1% of chitosan has been immobilized on bentonite.

XRD analysis

Figure 6 illustrates the XRD pattern of bentonite, chitosan, CIB, and crosslinked CIB beads. A typical 2θ peak for bentonite was detected at 6.42° that corresponds to basal spacing of 1.36 nm for (001) plane. Another characteristic 2θ peak of bentonite is found at 9.22°, which corresponds to a basal spacing of 0.95 nm. No significant shift in the diffraction angle of bentonite was observed on addition of chitosan and the crosslinking agents EDGE, GLA, and ECH,

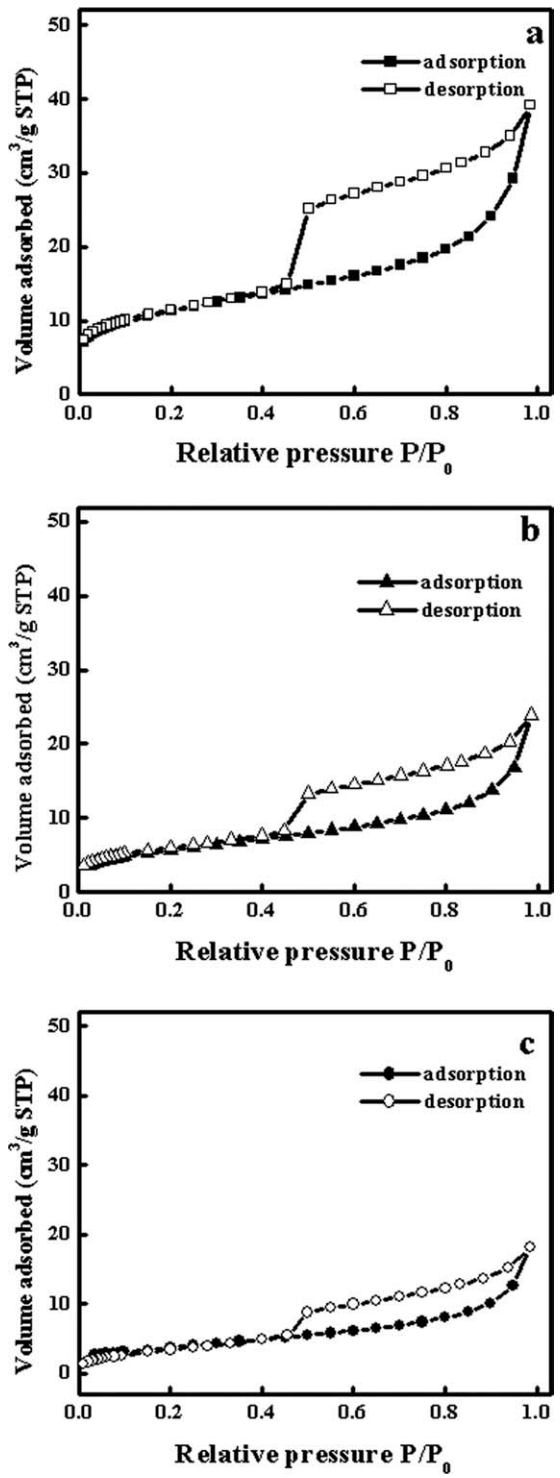

Figure 2 Isotherm plot of N_2 adsorption and desorption on (a) CIB-ECH, (b) CIB-EGDE, and (c) CIB-GLA beads.

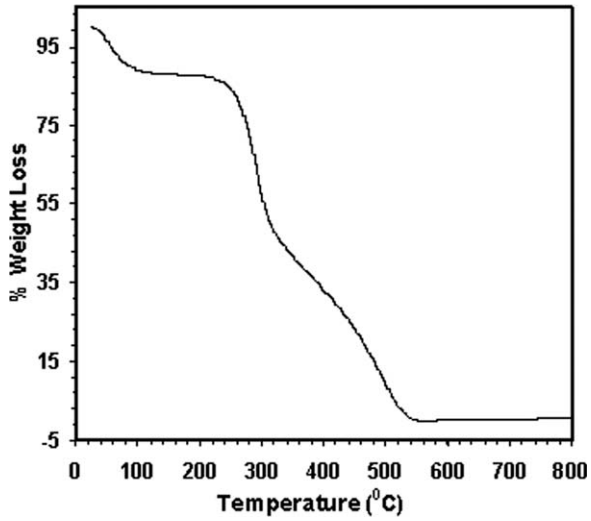

Figure 3 Thermogravimetric curve of chitosan.

which indicates the absence of chitosan and crosslinking agents intercalating into the interlayer of bentonite. The chitosan-clay ratio used in this study is 0.025 : 1, where the amount of chitosan was very low to cause observable intercalations. Shifts in basal spacing for CIB, CIB-EDGE, CIB-ECH, and CIB-GLA are within the range of 0.01 and 0.20 nm, which could be attributed to moisture and not intercalation.

In addition, the XRD intensity of bentonite at peak 6.42° was observed to decrease on addition chitosan and crosslinking agents. The interaction between bentonite and chitosan plus the crosslinking agents, taking into account the different molecular sizes and chemical structures, caused the distortion of the intrinsic lattice arrangement of bentonite, leading to a decrease in its crystallinity, which caused a decrease in peak intensity.

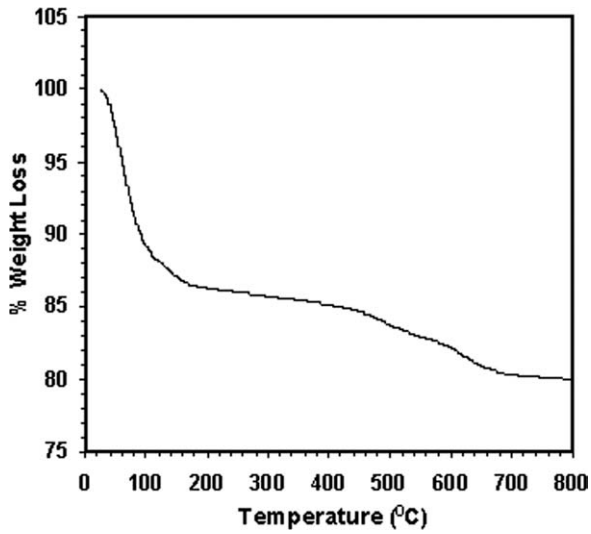

Figure 4 Thermogravimetric curve of bentonite.

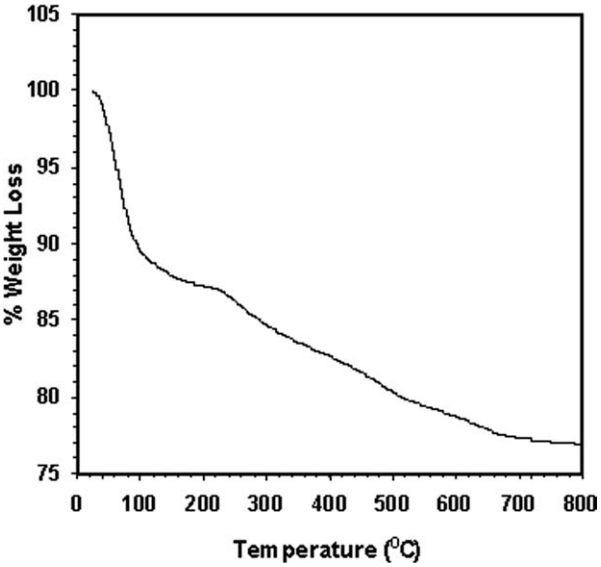

Figure 5 Thermogravimetric curve of CIB.

Effect of contact time and initial concentration

As shown in Figure 7, the adsorption of Cu(II) ions using CIB, CIB-ECH, CIB-EDGE, and CIB-GLA occurred rapidly. Cu(II) adsorption increased with contact time and attained equilibrium at 120 min for all four adsorbent beads. The adsorption capacity, q_e of CIB, CIB-ECH, CIB-EDGE, and CIB-GLA was observed to increase with initial concentration. A high initial concentration means an increase in the driving force caused by the concentration gradient and mass transfer effects, resulting to an increase in q_e values.[9] The order of the q_e values using the four modified adsorbents was as follows: CIB-EDGE $\sim$ CIB-ECH $>$ CIB $>>$ CIB-GLA. The adsorption capacity of CIB, CIB-EDGE and CIB-ECH are similar in values at initial concentration of 100 and 500 mg L^{-1}. However, the q_e values of CIB are lower than

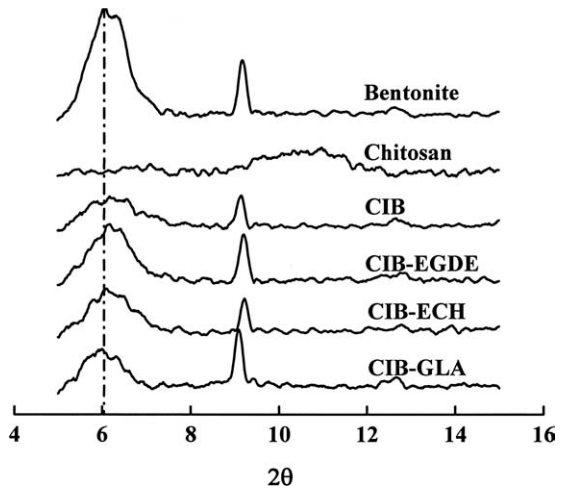

Figure 6 XRD patterns of bentonite, chitosan, CIB beads, CIB-EGDE beads, CIB-ECH beads, and CIB-GLA beads.

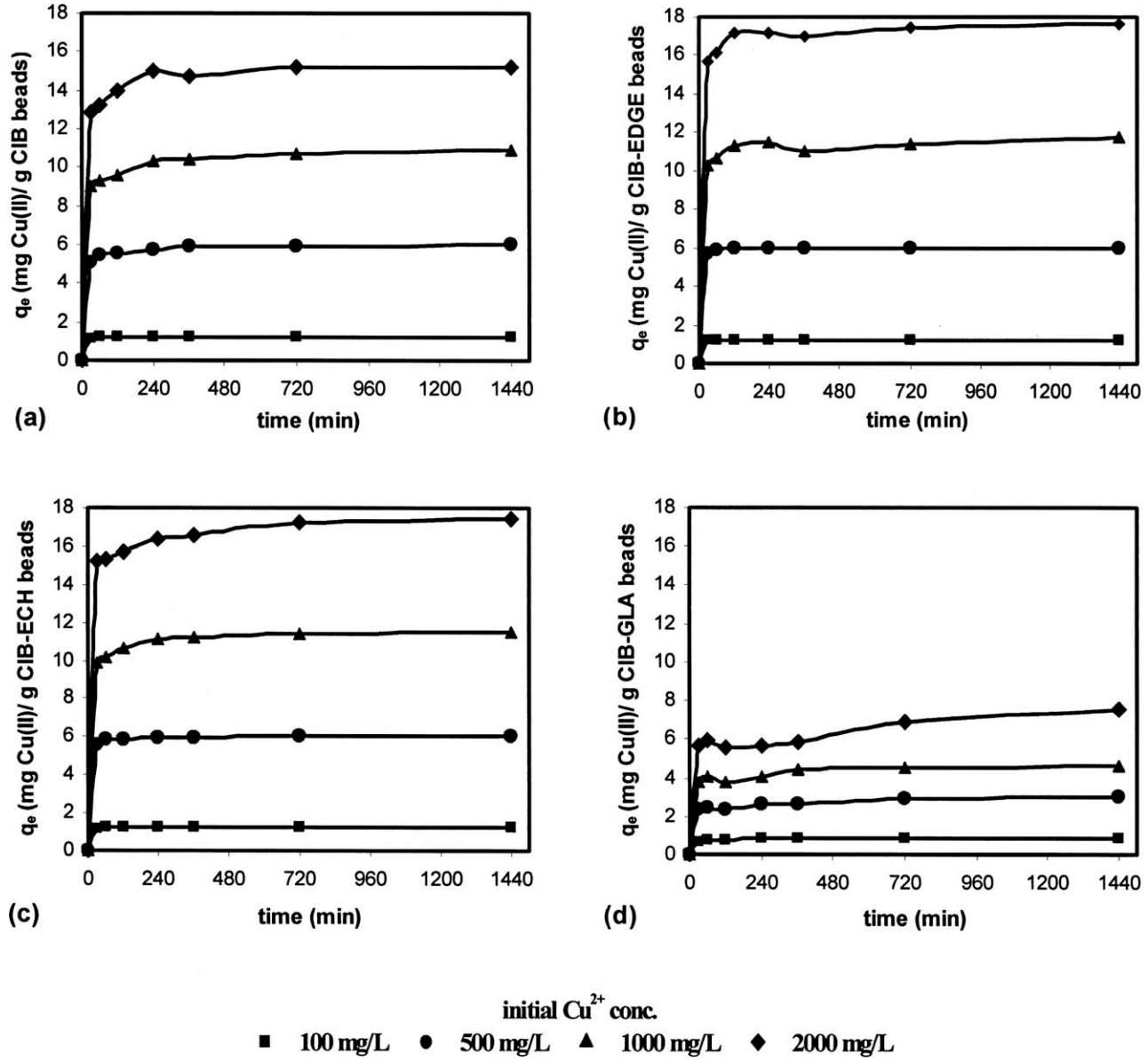

Figure 7 Adsorption capacity (q_e) of Cu(II) on (a) CIB, (b) CIB-EGDE, (c) CIB-ECH, and (d) CIB-GLA beads in terms of time and initial Cu(II) concentration at pH 4.

the two adsorbents at higher concentrations despite the slightly higher surface area of CIB beads over CIB-EDGE and CIB-ECH. At 1000 mg L^{-1} and above, the binding sites of CIB are almost saturated while CIB-EDGE and CIB-ECH can still adsorb more Cu(II) ions. Both EDGE and ECH contain additional hydroxyl groups found along its chain that serve as additional binding sites for Cu(II) ions. Among the modified adsorbents, GLA provided the lowest adsorption capacity for Cu(II) removal. GLA is a crosslinker in the dialdehyde group where it interacts with the amino ($-NH_2$) group of chitosan. The amino group of chitosan is one of the primary binding sites for heavy metals, therefore, using GLA reduced the number of binding sites for Cu(II) ions. Additionally, CIB-GLA has a low surface area available for adsorption, with properties like lower swelling capacities and a more hydrophobic character, which further contributed to its low adsorption capacities.[23]

CIB-ECH and CIB-EDGE have very similar adsorption capacity for Cu(II) removal. Both crosslinking agents belong to the epoxide group, where both contribute additional hydroxyl (—OH) groups that will serve as binding sites for Cu(II) ions.[24] Specifically, the ECH chain contains one hydroxyl group while the EDGE chain contains two hydroxyl groups along its structure that could serve as binding sites for Cu(II) ions. EDGE interacts with chitosan via its amino groups while ECH interacts with the hydroxyl group of chitosan. Hence, ECH may contain less hydroxyl group than EDGE but it leaves

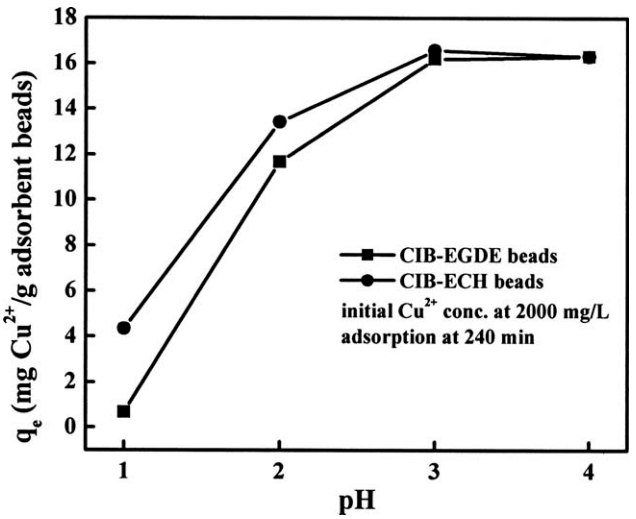

Figure 8 Effect of pH on the adsorption capacity (q_e) of Cu(II) ions onto CIB-EGDE and CIB-ECH beads.

the amino groups of chitosan to interact freely with Cu(II) ions. In addition, the ECH molecule is shorter, resulting to a more rigid polymeric chain, which reduces the affinity of Cu(II) ions to interact with the binding sites of CIB-ECH over the longer molecule of CIB-EDGE.[23] Taking into account all of these properties of ECH and EDGE led to the similar adsorption capacities for Cu(II) removal from aqueous solution.

Effect of pH

The effect of pH on Cu(II) adsorption using CIB-EDGE and CIB-ECH at an initial concentration of 2000 mg L^{-1} was investigated. Based on the results from previous section, CIB-EDGE and CIB-ECH provided maximum adsorption capacity over CIB and CIB-GLA. Therefore, CIB-EDGE and CIB-ECH were the adsorbents utilized in the study for effect of pH as well as the regeneration study. Figure 8 illustrates the adsorption capacity of Cu(II) ions onto CIB-EDGE and CIB-ECH beads at different pH values. The adsorption capacity of both adsorbent increased when the pH was increased from pH 1 to 4. The maximum adsorption capacity for the two adsorbent beads occurred at pH 4. The adsorption capacities of the adsorbent beads were very low at acidic pH since more H^+ are available to protonate the amine groups of chitosan, forming $-NH_3^+$. This in turn, reduces the binding sites available for the Cu(II) ions. In addition, the positive charge of $-NH_3^+$ exerts a high electrostatic repulsive force, which prevents the Cu(II) ions from approaching the adsorbent surface. Hence, at very low pH condition, the adsorption capacity was reduced.[25,26]

The surface charge of clay is also affected under acidic conditions. At very low pH, the aluminol and silanol groups (—MO) found on the clay surface becomes protonated.[26] In addition, the oxygen atoms on the surface interact with the water in acidic solution to form aqua complexes as shown by eq. (3):

$$\text{—— MO} + \text{H —— OH} \rightarrow \text{M —— } OH_2^+ + OH^- \quad (3)$$

The positive clay surface charge interacts repulsively with the approaching Cu(II) ions and prevents them from reaching the adsorbent surface. As a result, the adsorption capacity at low pH was further reduced.

At around pH3 and pH4, the inhibitory effect of H^+ decreases, which led to an increase in the Cu(II) adsorption capacity. Moreover, the amount of H^+ was reduced in comparison to the amount of Cu(II), therefore, Cu(II) can compete with H^+ to react with R-NH_2, which represents the chitosan chain with its amino group as shown in the eq. (4).[27]

$$R - NH_3^+ + Cu^{2+} \leftrightarrow R - NH_2Cu^{2+} + H^+ \quad (4)$$

Adsorption kinetics study

To investigate the mechanism of Cu(II) adsorption and to identify the rate-determining step, the pseudofirst-order and pseudosecond-order equations were applied to analyze the kinetic data.

The pseudofirst-order equation is given by eq. (5):

$$\log(q_e - q_t) = \log q_e - \frac{k_1}{2.303} t \quad (5)$$

where q_e and q_t (mg g^{-1}) are the adsorption capacities at equilibrium and at time t (min), respectively, and k_1 is the rate constant of the first-order adsorption (1 min^{-1}).[28] Plotting $\log(q_e - q_t)$ against t will give the pseudofirst-order kinetic rate constant, k_1 and the theoretical value of q_e.

The pseudosecond-order kinetic model was illustrated as eq. (6):

$$\frac{t}{q_t} = \frac{1}{k_2 q_e^2} + \frac{1}{q_e} t \quad (6)$$

where k_2 is the rate constant of adsorption (g mg^{-1} min). The straight line plot of t/q_t against t will give the value of the kinetic rate constant, k_2 and the theoretical value of q_e.

Based on Table II, the adsorption of Cu(II) using CIB, CIB-ECH, CIB-EDGE, and CIB-GLA did not fit the pseudofirst-order equation, owing to its low correlation coefficient values: $0.9005 < R^2 < 0.9541$, $0.9245 < R^2 < 0.9746$, $0.8688 < R^2 < 0.9746$, and $0.8105 < R^2 < 0.9537$, respectively. The pseudofirst order applies to a reversible reaction with the equilibrium being established between the solid and liquid phases.[17] The four modified adsorbent

TABLE II
Kinetic Parameters for Cu(II) Adsorption onto Non-Crosslinked and Crosslinked Chitosan Immobilized on Bentonite Beads

Adsorbent	Initial Cu(II) concentration (mg L^{-1})	Pseudofirst-order kinetic			Pseudosecond-order kinetic		
		R^2	k_1 (L min^{-1})	q_e (mg g^{-1})	R^2	k_2 (g mg^{-1} min)	q_e (mg g^{-1})
CIB	500	0.9005	0.0378	3.47	0.9881	0.0152	6.15
	1000	0.9182	0.0454	6.62	0.9763	0.0082	10.65
	2000	0.9541	0.0435	10.42	0.9857	0.0058	15.43
CIB-EGDE	500	0.8688	0.0412	2.08	0.9995	0.0558	6.12
	1000	0.9746	0.0426	6.63	0.9991	0.0169	11.72
	2000	0.9647	0.0567	12.63	0.9978	0.0093	17.99
CIB-ECH	500	0.9245	0.0493	3.70	0.9961	0.0205	6.40
	1000	0.9731	0.0500	7.34	0.9965	0.0118	11.42
	2000	0.9269	0.0541	8.48	0.9963	0.0100	16.72
CIB-GLA	500	0.8105	0.0362	1.02	0.9989	0.0930	2.60
	1000	0.9537	0.0408	2.34	0.9988	0.0407	4.24
	2000	0.8270	0.0410	1.96	0.9987	0.0575	6.04

beads follow the pseudosecond-order equation, given by its high correlation coefficient values ($R^2 > 0.9763$). The pseudosecond-order equation implies that chemisorption is the rate-determining step of the adsorption process. It signifies that the overall rate of Cu(II) adsorption process appears to be controlled by the chemical attachment and not by mass transport.[20] The adsorption mechanism may involve valency forces through sharing of electrons between Cu(II) and adsorbent beads.[26,29] A high adsorption capacity with short equilibrium time indicates a high degree of affinity between the Cu(II) and adsorbent beads.[20]

Adsorption isotherm study

The equilibrium isotherm is essential in describing the interaction between the Cu(II) ions and the adsorbent beads at a constant temperature. In this study, the experimental data were analyzed using the two isotherm equations, namely Langmuir and Freundlich model. The Langmuir model assumes that the solute is adsorbed on a finite number of binding sites with the same energy levels found on a homogenous surface. Langmuir isotherm is described as adsorption occurring on a monolayer surface coverage where there is no net interaction between adsorbed molecules.[28] The Langmuir equation is represented by eq. (7):

$$q_e = \frac{K_L C_e}{1 + bC_e} = \frac{C_{\max} b C_e}{1 + bC_e} \tag{7}$$

where q_e is the equilibrium Cu(II) loading on the adsorbent beads, C_e the equilibrium concentration of Cu(II), $C_{\max}$ the maximum capacity at monolayer coverage, and b is the relative energy (intensity) of adsorption, also known as binding constant.[26] The Freundlich model is based on an empirical equation. It is usually applied to adsorption of solute on active sites with heterogenous energy levels on rough surfaces and is given by eq. (8):

$$q_e = K_F C_e^{1/n} \tag{8}$$

where K_F and n are Freundlich constants related to relative adsorption capacity and adsorption intensity of the adsorbent, respectively.[29]

Based on Table III, CIB, CIB-ECH, and CIB-EDGE best fits the Langmuir isotherm with high correlation coefficient values ($R^2 > 0.99$). This implies that Cu(II) ions form a monolayer coverage on the homogenous surface of the adsorbent. On the other hand, CIB-GLA fitted very well with the Freundlich isotherm ($R^2 = 0.999$), which implies the occurrence of multisite adsorption of the Cu(II) ions on the surface with heterogenous energetic distributions.

TABLE III
Adsorption Isotherm Constants and Correlate Ion Coefficients of Cu(II) Adsorption on Crosslinked Chitosan Immobilized on Bentonite at pH 4

Adsorbents	Langmuir isotherm				Freundlich isotherm		
	R^2	K_L (L g^{-1})	b (L mg^{-1})	$C_{\max}$ (mg g^{-1})	R^2	K_F	n
CIB	0.991	22.727	2.307	9.85	0.932	3.221	3.83
CIB-EGDE	0.996	45.228	4.299	10.52	0.953	4.150	3.89
CIB-ECH	0.998	44.623	3.799	11.75	0.932	4.311	4.13
CIB-GLA	0.984	0.044	0.011	4.17	0.999	0.152	1.89

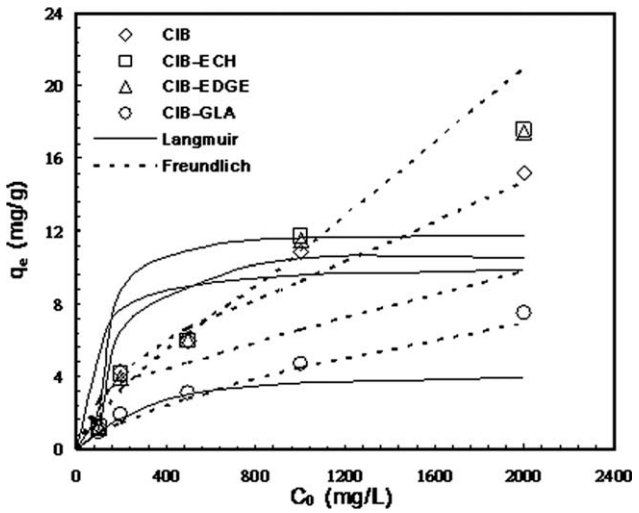

Figure 9 Experimental data points of Cu(II) using CIB, CIB-ECH, CIB-EDGE, and CIB-GLA fitted with the nonlinear plot of Langmuir and Freundlich model.

In Figure 9, the experimental data are plotted against the nonlinear plots generated by the Langmuir and Freundlich model. The simulated plot using the Freundlich isotherm agreed well with the experimental data points of Cu(II) adsorbed using CIB-GLA. On the other hand, the experimental data points using CIB, CIB-ECH, and CIB-EDGE illustrate a good fit to the nonlinear plots based on the Langmuir isotherm. This result agrees with the obtained correlation coefficient values (R^2) listed in Table III.

Based on the Langmuir isotherm, the C_{max} of Cu(II) on CIB, CIB-EGDE, CIB-ECH, and CIB-GLA beads were 9.85, 10.52, 11.75, and 4.17 mg g^{-1}, respectively. CIB-EDGE and CIB-ECH have high constant b values over CIB and CIB-GLA, an indication of high affinity of Cu(II) ions for the binding sites on the surface of the modified beads. This in turn causes the maximum monolayer adsorption values of Cu(II) to be arranged in the following order: CIB-ECH $\sim$ CIB-EDGE $>$ CIB $\gg$ CIB-GLA beads.

The Freundlich parameter constant, n, indicates the favorability of the adsorption. If the n value is less than 1, the adsorption intensity is favorable over the entire range of concentration used, but an n value of more than 1 means it is favorable only at high concentration. The adsorption intensity, n, for all four adsorbent beads is greater than 1, which indicates the adsorption is favorable only at high concentration.[1] The superior n values of CIB-ECH and CIB-EDGE over CIB and CIB-GLA means an enhanced intensity of the adsorption of Cu(II) ions, which led to higher values of the relative adsorption capacity, K_F.

The adsorption capacity of CIB-EDGE and CIB-ECH developed by this study was compared to chitosan, its modified forms and other biosorbents. As seen in Table IV, this study obtained a good maximum adsorption capacity for CIB-EGDE and CIB-ECH when compared to similar chitosan immobilization studies.[9,11,33] In addition, the adsorption capacity of CIB-ECH and CIB-EDGE obtained in this study is comparable to that of chitosan and higher than bentonite and other natural adsorbents such as tobacco, coconut, bark, and sugarcane.[30,32,34–36] This indicates the potential of the aforementioned adsorbents in large-scale practical application.

Desorption and regeneration study

The recovery of the metal adsorbed and the regeneration of adsorbent beads are important in determining the reusability of the adsorbent material. In this study, CIB-ECH and CIB-EDGE beads underwent

TABLE IV
Comparative Adsorption Capacity and Kinetics of Cu(II) Ions onto Various Bioadsorbents

Adsorbent	Adsorption capacity (mg g^{-1})	Adsorption kinetics (fitting model)	BET surface area (m^2 g^{-1})	References
CIB-EGDE	10.5	Pseudosecond order	20.18	This study
CIB-ECH	11.6	Pseudosecond order	38.96	This study
CIB-GLA	4.2	Pseudosecond order	13.45	This study
CIB	9.9	Pseudosecond order	39.17	This study
Chitosan	16.8	Pseudosecond order	NA	30
Epichlorohydrin crosslinked chitosan (CCTS)	16.8	Pseudosecond order	NA	31
Bentonite	7.94	NA	NA	32
CHB (chitosan-immobilized on bentonite)	21.55	Pseudosecond order	33.17	11
CCB (chitosan-coated bentonite)	12.21	Pseudosecond order	48.31	33
CCB-ECH	9.43	Pseudosecond order	37.14	33
CCS (chitosan-coated sand)	8.76	Pseudosecond order	39.78	9
Sugar cane, bagasse	0.3	NA	NA	34
Coconut, shell	2.6	NA	NA	34
Kudzu, bark	8.2	NA	NA	34
Tobacco, bark	14.3	NA	NA	34

NA: not available

TABLE V
Desorption of Cu(II) from CIB-EGDE and CIB-ECH Beads Using Deionized Water (pH 7) and HCl Solution at pH 1 and pH 3

		CIB-EDGE beads			CIB-ECH beads		
Desorption solution	Initial Conc. (mg L^{-1})	Cu(II) ions adsorbed (mg L^{-1})	Cu(II) ions desorbed (mg L^{-1})	% desorption	Cu(II) ions adsorbed (mg L^{-1})	Cu(II) ions desorbed (mg L^{-1})	% desorption
HCl (pH = 1)	100	100	95.05	95.05	99.96	76.96	76.99
	500	498.08	461.77	92.71	498.45	411.77	82.61
	1000	910.75	906.56	99.54	904.27	773.33	85.52
	2000	1359.30	1347.34	99.12	1358.87	1214.69	89.39
HCl (pH = 3)	100	100	0.00	0.00	100	0.14	0.14
	500	486.09	0.00	0.00	473.78	0.05	0.01
	1000	915.67	6.04	0.66	879.04	1.76	0.20
	2000	1352.90	61.29	4.53	1329.52	35.10	2.64
Tap water (pH = 7)	100	100	0.00	0.00	100	0.03	0.03
	500	475.01	0.00	0.00	468.90	0.70	0.15
	1000	891.98	1.43	0.16	897.34	2.87	0.32
	2000	1267.98	1.14	0.09	1298.56	39.74	3.06

one desorption and regeneration cycle using deionized water (pH 7), and HCl solution (pH 1 and pH 3). The desorption study using solution with pH 3 and pH 7 was performed to test the stability of the CIB-EGDE and CIB-ECH beads in capturing Cu(II) ions. The desorption study using solution at pH 1 was performed to investigate the strength of adsorbent beads, the potential recovery of Cu(II) ions, and the reusability of the adsorbent beads.

According to Table V, after the desorption cycle using HCl (pH 3) and tap water (pH 7), it is observed that there is very low recovery of Cu(II) ions (% desorption $<$ 4.53% for pH 3 and % desorption $<$ 3.06% for pH 7) for CIB-EDGE and CIB-ECH. This indicates the stability of Cu(II) ions adsorbed under slightly acidic and neutral conditions. Desorption using CIB-EDGE beads at pH 1 resulted to a high recovery of Cu(II) ions (%desorption $>$ 92%), which displays the probability of recovering the adsorbed Cu(II) ions. However, the CIB-ECH beads has lower % recovery values in comparison with the CIB-EDGE beads, indicating a stronger bond formed between Cu(II) ions and the CIB-ECH beads.

After desorption, the two adsorbent beads, CIB-EGDE and CIB-ECH, were reused for a second cycle of Cu(II) adsorption. The results in Table VI showed that the adsorption capacity of the regenerated CIB-EDGE beads (at pH 1) are very low, where the % adsorption $<$2%. However, regenerated CIB-ECH beads using pH 1 have slightly higher % adsorption values, owing to its greater mechanical strength and chemical stability over CIB-EDGE beads. This indicates that CIB-ECH beads provide better efficiency for reuse than CIB-EGDE beads Although using HCl solution (pH 1) for desorption contributed the greatest recovery of Cu(II) for the beads, it also destroyed the adsorbents' physical structure, leading to the dissolution of the CIB-ECH and CIB-EGDE beads. As a result, regeneration provided very low adsorption capacity. Using desorption agents at pH 3 and pH 7

TABLE VI
Adsorption Data of Cu(II) Removal Using Regenerated CIB-EGDE and CIB-ECH Beads After One Desorption Cycle Using Deionized Water (pH 7) and HCl Solution (pH 1 and pH 3) at Equilibrium Contact Time (240 min)

		CIB-EDGE beads			CIB-ECH beads		
Desorption solution	Initial conc. (mg L^{-1})	C_e (mg L^{-1})	q_e (mg g^{-1})	% adsorption	C_e (mg L^{-1})	q_e (mg g^{-1})	% adsorption
HCl (pH = 1)	100	93.95	0.07	2.02	57.11	0.51	42.89
	500	498.75	0.04	0.65	363.37	1.64	27.33
	1000	998.03	0.02	0.20	806.33	2.32	19.37
	2000	2002.67	0.00	0.00	1749.73	3.00	12.51
HCl (pH = 3)	100	0.01	1.20	99.99	0.01	1.20	99.99
	500	26.40	5.68	94.72	19.88	5.76	96.02
	1000	390.85	7.31	60.92	297.95	8.42	70.21
	2000	1519.00	5.77	24.05	1334.33	7.99	33.28
Tap water (pH = 7)	100	0.01	1.20	99.99	0.01	1.20	99.99
	500	16.42	5.80	96.72	16.15	5.81	96.77
	1000	324.57	8.10	67.54	328.60	8.06	67.14
	2000	1430.67	6.83	28.47	1354.20	7.75	32.29

exhibited low percent desorption. However, the adsorbent beads still could be used for another adsorption cycle but with lower adsorption capacity.

CONCLUSIONS

In this study, the removal of Cu(II) ions from aqueous solution using noncrosslinked and crosslinked CIB beads was examined under batch conditions. The adsorption capacities for Cu(II) removal are arranged in the following order: CIB-EGDE > CIB-ECH > CIB > CIB-GLA. An increase in the adsorption capacity of the adsorbent beads was observed at higher initial concentration and as the solution pH was increased from pH 1 to 4. Under equilibrium conditions, the adsorption isotherm of CIB, CIB-EGDE, and CIB-ECH beads could be well fitted using the Langmuir isotherm, which describes monolayer coverage on a homogeneous adsorbent surface. On the other hand, adsorption using CIB-GLA beads correlated well with the Freundlich isotherm. Moreover, the overall kinetic data was best described by the pseudosecond-order equation, which suggests that chemisorption is the rate-determining step. About 92 and 75% of Cu(II) ions could be desorbed from CIB-EDGE and CIB-ECH using HCl solution (pH 1) at a contact time of 240 min. In general, the results of this study illustrate the possibility of using CIB-EDGE and CIB-ECH as possible material for PRBs in the treatment of acidic plumes and contaminated groundwater.

References

1. Ngah, W. S.; Fatinathan, S. Chem Eng J 2008, 143, 62.
2. Anirudhan, T. S.; Rijith, S. Colloids Surf A 2009, 351, 52.
3. Han, R.; Zou, L.; Zhao, X.; Xu, Y.; Xu, F.; Li, Y.; Wang, Y. Chem Eng J 2009, 149, 123.
4. Juang, R. S.; Shao, H. J. Water Resour 2002, 36, 2999.
5. Low, K. S.; Lee, C. K.; Leo, A. C. Bioresour Technol 1995, 51, 227.
6. Marshall, W. E.; Johns, M. M. J Chem Technol Biotechnol 1996, 66, 192.
7. Wan, M. W.; Petrisor, I. G.; Lai, H. T.; Kim, D.; Yen, T. F. Carbohydr Polym 2004, 55, 249.
8. Gecol, H.; Ergican, E.; Miakatsindila, P. J Colloid Interface Sci 2005, 197, 165.
9. Wan, M. W.; Kan, C. C.; Rogel, B. D.; Dalida, M. L. Carbohydr Polym 2010, 80, 891.
10. Futalan, C.; Kan, C. C.; Dalida, M. P.; Pascua, C.; Wan, M. W. Carbohydr Polym 2011, 83, 697.
11. Futalan, C.; Kan, C. C.; Dalida, M. P.; Hsien, K. L.; Pascua, C.; Wan, M. W. Carbohydr Polym 2011, 83, 528.
12. Veera, M. B.; Krishnaiah, A.; Jonathan, L. T.; Edgar, D. S. Environ Sci Technol 2003, 37, 4449.
13. Popuri, S. R.; Vijaya, Y.; Boddu, V. M.; Abburi, K. Bioresour Technol 2009, 100, 194.
14. Vijaya, Y.; Popuri, S.; Boddu, V.; Krishnaiah, A. Carbohydr Polym 2008, 72, 261.
15. Tamura, A.; Satoh, E.; Kashiwada; A.; Matsuda, K.; Yamada, K. J Appl Polym Sci 2010, 115, 137.
16. Bhattacharyya, K. G.; Gupta, S. S. Adv Colloid Interface Sci 2008, 140, 114.
17. Kamari, A.; Ngah, W. S. Colloids Surf B 2009, 73, 257.
18. Wan Ngah, W. S.; Ghani, S. A.; Kamari, A. Bioresour Technol 2005, 96, 443.
19. Ngah, W. S. W.; Endud, C. S.; Mayanar, R. React Funct Polym 2002, 50, 181.
20. Chiou, M. S.; Li, H. Y. Chemosphere 2003, 50, 1095.
21. Wang, S. F.; Shen, L.; Tong, Y. J.; Chen, L.; Phang, I. Y.; Lim, P. Q.; Liu, T. X. Polym Degrad Stab 2005, 90, 123.
22. Joshi, G. V.; Kevadiya, B. D.; Patel, H. A.; Bajaj, H. C.; Jasra, R. V. Int J Pharm 2009, 374, 53.
23. Guibal, E. Sep Purif Technol 2004, 38, 43.
24. Machado, M. O.; Lopes, E.; Sousa, K. S.; Airoldi, C. Carbohydr Polym 2009, 77, 760.
25. Jin, L.; Bai, R. Langmuir 2002, 18, 9765.
26. Sankararamakrishnan, N.; Sharma, A. K.; Sanghi, R. J Hazard Mater 2007, 148, 353.
27. Václaviková, M.; Gallios, G. P. Acta Montanistica Slovaca 2006, 11, 393.
28. Wan Ngah, W. S.; Hanafiah, M. A. K. M.; Yong, S. S. Colloids Surf B 2008, 65, 18.
29. Gupta, S. S.; Bhattacharyya, K. G. J Environ Manage 2008, 87, 46.
30. Huang, C.; Chung, Y. C.; Ming, R. L. J Hazard Mater 1996, 45, 265.
31. Tan, S.; Wang, Y.; Peng, C.; Tang, Y. J Appl Polym Sci 1999, 71, 2069.
32. Kapinar, N.; Donat, R. Desalin 2009, 249, 123.
33. Dalida, M. L. P.; Mariano, A. F. V.; Futalan, C. M.; Kan, C. C.; Tsai, W. C.; Wan, M. W. Desalin 2011, 275, 154.
34. Demirbas, A. J Hazard Mater 2008, 157, 220.
35. Chen, A. H.; Liu, S. C.; Chen, C. Y.; Chen, C. Y. J Hazard Mater 2008, 154, 184.
36. Ho, Y. S. J Hazard Mater 2006, 136, 681.